Cellular Signalling 24 (2012) 1116–1125

Contents lists available at SciVerse ScienceDirect

Cellular Signalling

journal homepage: www.elsevier.com/locate/cellsig

Low-power laser irradiation (LPLI) promotes VEGF expression and vascular endothelial cell proliferation through the activation of ERK/Sp1 pathway

Jie Feng, Yingjie Zhang, Da Xing *

MOE Key Laboratory of Laser Life Science & Institute of Laser Life Science, College of Biophotonics, South China Normal University, Guangzhou 510631, China

ARTICLE INFO

Article history:
Received 22 November 2011
Received in revised form 10 January 2012
Accepted 26 January 2012
Available online 2 February 2012

Keywords:
Angiogenesis
LPLI
Sp1
ERK
VEGF
Proliferation

ABSTRACT

Angiogenesis, the growth of new blood vessels from pre-existing vessels, represents an excellent therapeutic target for the treatment of wound healing and cardiovascular disease. Herein, we report that LPLI (low-power laser irradiation) activates ERK/Sp1 (extracellular signal-regulated kinase/specificity protein 1) pathway to promote VEGF expression and vascular endothelial cell proliferation. We demonstrate for the first time that LPLI enhances DNA-binding and transactivation activity of Sp1 on VEGF promoter in vascular endothelial cells. Moreover, Sp1-regulated transcription is in an ERK-dependent manner. Activated ERK by LPLI translocates from cytoplasm to nuclear and leads to increasing interaction with Sp1, triggering a progressive phosphorylation of Sp1 on Thr453 and Thr739, resulting in the upregulation of VEGF expression. Furthermore, selective inhibition of Sp1 by mithramycin-A or shRNA suppresses the promotion effect of LPLI on cell cycle progression and proliferation, which is also significantly abolished by inhibition of ERK activity. These findings highlight the important roles of ERK/Sp1 pathway in angiogenesis, supplying potential strategy for angiogenesis-related diseases with LPLI treatment.

1. Introduction

Angiogenesis is an important physiological process involved in developmental and pathological vascularization, such as ischemia, wound repair and cardiovascular disease [1–3]. Although these models showing different kinetics and growth factor requirements recapitulate distinct physiological responses, they share common features: activation of the proliferation, migration and tube formation programs of endothelial cells which serve as both the protective inner lining of vessels and the local site for delivery of oxygen to all tissues. Plenty of physical or chemical factors exert their effects on angiogenesis through regulating various endothelial cell activities, including proliferation, survival, migration or tube formation [4–6].

Low-power laser irradiation (LPLI) with light spectrum from the visible to near-infrared range is a non-damage physical therapy. A growing body of experimental and clinical studies have demonstrated that LPLI regulates cell survival, proliferation, and differentiation [7–12], which contributes LPLI to receive increasing attention in the treatment of various pathological progresses, including oral mucositis, stroke, wound healing, inflammation, Alzheimer's disease and angiogenesis [13–18]. Therefore, the effect of LPLI on endothelial cell proliferation may provide potential therapeutic strategy for angiogenesis. However, the underlying mechanisms are not fully elucidated.

It has been reported that specificity protein 1 (Sp1) acts as a G1 cell cycle phase special transcription factor in epithelial cells [19], and another study also shows that the activation of cyclinD1 promoter in vascular endothelial cells largely depends on the Sp1 sites, mediated by the Ras-dependent pathway [20], indicating that Sp1 may play important roles in endothelial cell proliferation.

Sp1, as the first mammalian transcription factor to be cloned, belonging to the Sp and Krüppel-like factor (Sp/KLF) family [21], has been attested to regulate the expression of thousands of genes implicated in an array of cellular processes, such as cell growth, proliferation, and angiogenesis in response to physiologic and pathological stimuli [22–24]. It contains a prototypic Cys2/His2-type zinc finger motif, through which it binds directly to the GC box element of DNA to activate or repress gene transcription [25–27]. Vascular endothelial growth factor (VEGF), one of the most important angiogenic switch molecular, exerts great function on the behaviors of endothelial cells, including migration, proliferation, and differentiation [28]. The high GC-rich motifs in the proximal regions of VEGF promoter are regulated by Sp1 [29].

Sp1-dependent transcription can be regulated by a variety of signals through alterating Sp1 abundance, DNA binding activity, and/or transactivation activity which is influenced by a series of posttranslational

Abbreviations: HUVEC-CS, human umbilical vein endothelial cells subline; HEK 293T, human embryonic kidney 293T; LPLI, low-power laser irradiation; ERK, extracellular signal-regulated kinase; Sp1, specificity protein 1; VEGF, vascular endothelial growth factor; EGF, epidermal growth factor; MTA, mithramycin-A; PD, PD98059; Gö, Gö6983; PMSF, phenylmethylsulfonyl fluoride; YFP, yellow fluorescence protein; CFP, cyan fluorescence protein; FRET, fluorescence resonance energy transfer; FACS, flow cytometry assay; ChIP, chromatin immunoprecipitation; Co-IP, co-immunoprecipitation; WCL, whole cell lysate.

* Corresponding author. Tel.: +86 20 85210089; fax: +86 20 85216052.
E-mail address: xingda@scnu.edu.cn (D. Xing).

0898-6568/$ – see front matter © 2012 Elsevier Inc. All rights reserved.
doi:10.1016/j.cellsig.2012.01.013

modifications, especially phosphorylation [30,31] via protein kinases including extracellular signal-regulated kinase (ERK) [32,33], atypical protein kinase C-ζ (PKC-ζ) [34], Akt [35], cyclin-dependent kinase (CDK) [36], casein kinase II (CKII) [37], and DNA-dependent protein kinase [38].

In the present study, we demonstrate for the first time that LPLI stimulates ERK-dependent Sp1 activation, and the activation of ERK/Sp1 signaling pathway is crucial in the up-regulation of VEGF expression, which promotes cell cycle progression and proliferation. Our findings will extend the knowledge about the cellular signaling mechanisms mediating LPLI-induced proliferation, providing insight into establishing the therapeutic potential of LPLI for angiogenesis.

2. Materials and methods

2.1. Materials

Epidermal growth factor (EGF) (diluted in DMSO) was purchased from Pepro Tech (Rocky Hill, NJ). Cell Counting Kit-8 (CCK-8) was purchased from Dojindo Laboratories (Kumamoto, Japan). JetPEI™-HUVEC DNA transfection reagent was purchased from Polyplus-transfection (Bioparc, France). Lipofectamine™ 2000 reagent was purchased from Invitrogen (Carlsbad, CA). PD98059 (PD) and API-2 were purchased from Santa Cruz Biotechnology (Santa Cruz, CA). Mithramycin-A (MTA) was purchased from ENZO (Lausen, Switzerland). Gö6983 (Gö) was purchased from Merck (Darmstadt, Germany). The concentrations of EGF, PD, API-2, Gö and MTA used in our experiments were 50 ng/ml, 1 μM, 2 μM, 20 μM and 200 nM, respectively. The antibodies used for western blotting included antibodies against ERK, phospho-ERK (Cell Signalling Technology, Danvers, MA); phospho-Sp1 (Thr453) (Abcam plc, UK); phospho-Sp1 (Thr739) (Bioword Technology, Inc., USA); Sp1, VEGF, β-actin and Histone (Santa Cruz, CA). The plasmids pSp1-luc and mpSp1-luc reporters were kindly supplied by Prof. Shih-Ming Huang [39]. Sp1-shRNA nt1805 and non-targeting control Sp1-shRNA NT were kindly provided by Prof. Jane Azizkhan-Clifford [40]. CFP-Sp1 plasmid was a gift from Prof. Stephen Safe [41]. CFP-ERK, ERK-YFP and MEK-YFP plasmids were kindly provided by Prof. Michiyuki Matsuda [42].

2.2. Cell culture and transfection

Human umbilical vein endothelial cells subline (HUVEC-CS) was obtained from the Department of Life Science, University of Electronic Science and Technology of China. HUVEC-CS cells were then plated to gelatin-coated T75 flasks and grown to approximately 70% confluence for five more passages in MEM D-Val containing 20% FBS, 1 unit/ml penicillin, 1 μg/ml streptomycin and 4 μg/ml gentamicin [43,44]. Human embryonic kidney 293T (HEK 293T) cells were cultured in Dulbecco's modified Eagle's medium (DMEM, Life Technologies, Inc., Grand Island, NY) supplemented with 10% fetal bovine serum. Both of them were cultured in a humidified (5% CO_2, 37 °C) incubator. When the cells grew to 70–80% confluence, transfections were performed with 1 μg expression vectors using the jetPEI™-HUVEC for HUVEC-CS cells and Lipofectamine™ 2000 for HEK 293T cells according to the manufacturer's instructions in serum-free medium. The serum-free medium was replaced with fresh culture medium after 5 h and cells were incubated for an additional 24–48 h for expression.

2.3. Low-power laser irradiation

All groups of cells were starved for 24 h before irradiated with He–Ne laser (632.8 nm, 10 mW, 12.74 mW/cm^2, HN-1000, Guangzhou, China) and/or treated with different chemicals. The entire procedure was carried out at room temperature. Throughout each experiment, the cells were kept either in a complete dark or a very dim environment, except when subjected to light irradiation, to minimize the ambient light interference [17].

2.4. Cell viability assay

Cell viability was assessed with CCK-8 after laser irradiation. At the indicated times, CCK-8 was added and incubated for 1.5 h. OD450, the absorbance value at 450 nm, was read with a 96-well plate reader (DG5032, Huadong, Nanjing, China). The value is directly proportional to the number of viable cells in a culture medium.

2.5. Chromatin immunoprecipitation (ChIP) analysis

HUVEC-CS cells following indicated treatments were fixed in 1% formaldehyde for 10 min at 37 °C to cross-link protein complexes to the DNA. The reaction was stopped by the addition of glycine to a final concentration of 0.125 M for 5 min at room temperature. Cells were washed with cold PBS, scraped and lysed in SDS lysis buffer, and settled on ice for 10 min. Chromatin was sheared by sonication four times for 10 s, yielding DNA fragments of 200–1000 bp. Samples were then precleared with salmon sperm DNA protein A-Sepharose beads (Roche Applied Sciences, Indianapolis, IN) for 30 min with agitation, and one-tenth of the samples was set aside as an input control. The soluble chromatin fraction was collected and incubated overnight with 3 μg of anti-Sp1 antibody or control IgG antibody at 4 °C. The immunoprecipitates were pelleted by centrifugation and incubated at 65 °C to reverse the protein–DNA cross-linking. The DNA was extracted from the eluate by the phenol/chloroform method and then precipitated by ethanol [45]. The region from −272 to +18 bp of the VEGF promoter was amplified using the following primers: sense, 5′-CCGCGGGCGCGTGTCTCTGG-3′; antisense, 5′-TGCCCCAAG CCTCC GCGATCCTC-3′. PCR products were separated on a 1.5% agarose gel, stained with ethidium bromide, and visualized under UV light.

2.6. Luciferase assay

pSp1-luc and mpSp1-luc used in this study are plasmids containing three tandem repeats of consensus Sp1 sites and their corresponding mutant that drives luciferase gene. Luciferase activity was determined in cell lysates using the following method. Briefly, cells were transfected with pSp1-luc or mpSp1-luc, and then treated with indicated ways. Afterwards, culture medium was removed, and cells were washed with PBS and lysed (125 μl lysis buffer/well; 15% glycerol, 1% TritonX-100, 10 mM $MgCl_2$, 1 mM EDTA, 25 mM Tris–phosphate pH 7.8) for 10 min at 4 °C. Luciferase content in 100 μl cell lysate/well was injected 100 μl substrate [per 5 ml: 83 μl ATP disodium salt (50 mM; Sigma), 117 μl water, 1.5 ml D-luciferin sodium salt (1 mM in 10 mM Tris–phosphate, pH 7.8; Sigma), 3.3 ml lysis buffer]. Luciferase assay was conducted using a lucifererase assay system (Promega Corporation), and luminescence emission was determined over 2 s [46].

2.7. ERK-YFP translocation assay

To monitor ERK-YFP translocation in living cells, HUVEC-CS cells were transfected with pERK-YFP. After 36 h expression, cells were starved in serum-free medium for 24 h. Using LSM 510 confocal microscope (Carl Zeiss, Jena, Germany), we imaged the distribution pattern of ERK-YFP simultaneously after LPLI.

2.8. Cellular fractionation

To prepare cytoplasmic and nuclear fractions, cells were washed in ice-cold PBS, scraped, and homogenized in ice-cold hypotonic buffer (10 mM HEPES pH 7.4; 10 mM KCl; 1.5 mM $MgCl_2$; 1 mM EDTA; 1 mM DTT) containing 100 μg/ml phenylmethylsulfonyl fluoride (PMSF).

Cytoplasmic and nuclear fractions were obtained as described [17]. Then the cellular fractions were analyzed by western blot.

2.9. Western blot assay and co-immunoprecipitation (Co-IP)

For western blot assay, the cells were plated in 6-cm petri dishes. Briefly, the treated or untreated cells were harvested, washed with ice-cold PBS (pH 7.4), and lysed with ice-cold lysis buffer (50 mM Tris–HCl, pH 8.0, 150 mM NaCl, 1% Triton X-100, and 100 μg/ml PMSF) for 30 min on ice. The lysates were centrifuged at 12,000 rpm for 5 min at 4 °C, and the protein concentration was determined. Equivalent samples (40–100 μg of protein extract was loaded on each lane) were subjected to SDS-PAGE on 10% or 15% gel. The proteins were then transferred onto PVDF membranes and probed with the indicated antibodies, followed by secondary antibodies: goat anti-mouse conjugated to Alexa Fluor 800 or goat anti-rabbit conjugated to IRDyeTM 700. Detection was performed using the LI-COR Odyssey Infrared Imaging System (LI-COR, Inc., Lincoln, NE).

Cells were extracted in lysis buffer supplemented with protease inhibitor cocktail set I for 1 h on ice. After centrifugation, the supernatant was incubated with the indicated antibody at ambient temperature for 2 h and subsequently with protein A-Sepharose (50% slurry, Roche Applied Sciences, Indianapolis, IN) at 4 °C overnight and then were washed three times. The pellet was resuspended with the same volume of SDS sample buffer, and boiled to remove Sepharose beads. Then the whole cells lysates (WCL) and immunoprecipitates were analyzed by western blot [47,48].

2.10. Fluorescence resonance energy transfer (FRET) analysis

FRET was performed on a commercial laser scanning microscopes (LSM 510/ConfoCor2) combination system (Carl Zeiss, Jena, Germany). For excitation, the 458 nm line of an argon–ion laser was attenuated with an acousto-optical tunable filter, reflected by a dichroic mirror (main beam splitter HFT 458), and focused through a Plan-Neofluar 40×/1.3 NA oil DIC objective (Carl Zeiss) onto the sample. Cyan fluorescence protein (CFP) and YFP (FRET acceptor) emission were collected through 470–500 and 535–545 nm band pass filters, respectively. The quantitative analysis of the fluorescence images was performed using Zeiss Rel 3.2 image processing software (Carl Zeiss). After background subtraction, the average of fluorescence intensity per pixel was calculated. For time-lapse imaging, culture dishes were mounted onto the microscope stage that was equipped with a temperature-controlled chamber (Carl Zeiss, Jena, Germany) [47].

2.11. RNAi-mediated gene silencing

For RNAi-mediated gene silencing, we used Sp1-specific shRNA targeting nt1805 of Sp1 cDNA and non-targeting shRNA NT. Cells were assayed for gene silencing by western blot at 48 h post transfection.

2.12. Cell-cycle analysis

Cells harvested for 24 h were irradiated with He–Ne laser and/or treated with different chemicals. After 24 h incubation, cells were fixed with 70% ethanol, and pretreated with 250 μg/ml RNase. Quantitation of proliferation by propidium iodide (PI; 50 μg/ml) staining was performed. Flow cytometry assay (FACS) was performed on a FACS canto flow cytometer (Becton Dickinson, Mountain View, CA) with excitation at 488 nm. Cell cycle profile was determined by using the program M software on the flow cytometer.

2.13. Statistics

All assays were performed at least three times. All the error bars represented as the mean ± SEM (n = 5). For statistical evaluation Student's paired *t*-test was used and significance was defined as $P<0.05$. For fluorescence emission intensity analysis, a background subtraction was performed for all the data.

3. Results

3.1. LPLI enhances transcriptional activity of Sp1 dependent on ERK, but independent on PKC-ζ or Akt

To select an appropriate laser irradiation dose to induce proliferation, HUVEC-CS cells starved for 24 h were treated with a series of laser irradiation dose range from 0.3 to 2.1 J/cm^2. Then cell viability was detected using CCK-8 at 24 h following irradiation. The result showed that cell viability increased in a dose-dependent manner in LPLI-treated groups comparing with the non-treated cells (Fig. 1A). A significant increase was observed at the dose of 1.8 and 2.1 J/cm^2; meanwhile, to minimize thermal effect, 1.8 J/cm^2 was selected as the optimum irradiation dose in our following studies.

In order to confirm the effect of LPLI on Sp1-binding activity to VEGF promoter, we performed ChIP assay. Mithramycin-A (MTA) was used to competitively bind against Sp1 to GC-rich areas. Our data showed that LPLI promoted the binding activity of Sp1 to VEGF promoter, which was inhibited by MTA (Fig. 1B, C). To further investigate the effect of LPLI on Sp1 transactivation activity, we transiently transfected pSp1-luc or mpSp1-luc into HEK 293T cells. Relative luciferase activity showed an increase in LPLI-treated cells transfected with pSp1-luc and no obvious changes in cells transfected with mpSp1-luc (Fig. 1D), indicating LPLI enhanced transactivation activity of Sp1.

Sp1-dependent transcription is significantly influenced by its phosphorylation. To identify the kinases phosphorylating Sp1 upon LPLI, cells transfected with pSp1-luc plasmid were pretreated with ERK inhibitor PD98059 (PD), PKC inhibitor Gö6983 (Gö) and Akt inhibitor API-2 respectively before LPLI. LPLI increased transciptional activity of Sp1, which was reversed by pretreatment with PD, but not Gö and API-2 (Fig. 1E). This result suggested that LPLI potentially upregulated the phosphorylation of Sp1 through an ERK-dependent pathway.

3.2. LPLI induces ERK activation and its translocation from cytoplasm to nucleus

To further explore whether ERK can be activated responding to LPLI, we visualized the interaction between ERK and MEK by intermolecular FRET technique. MEK-YFP and CFP-ERK plasmids were co-transfected into cells. After 24 h starvation, the cells were treated with LPLI, and then the real-time CFP, FRET and the ratio of FRET/CFP fluorescence images were collected with LSM510 microscopy for 120 min. As it was revealing, the CFP fluorescence increased, while the FRET fluorescence decreased as well as the FRET/CFP ratio compared with control (Fig. 2A). The results verified that the interaction between ERK and MEK weakened gradually after LPLI, indicating ERK was activated following its dissociation from MEK. The result was further confirmed by the statistical analysis of fluorescence intensities (Fig. 2B, C).

In order to further elucidate whether ERK subcellular location changed by LPLI, we examined the translocation of ERK by transfecting YFP-ERK. Cells were brought to quiescence by withdrawal of serum for 24 h before LPLI. Upon LPLI stimulation, we observed a rapid increase of YFP-ERK in nucleus at about 30 min, which almost lasted for 90 min (Fig. 2D). Line-scan plots of these YFP-ERK images illustrated the subcellular location changes of ERK (Fig. 2E). The result

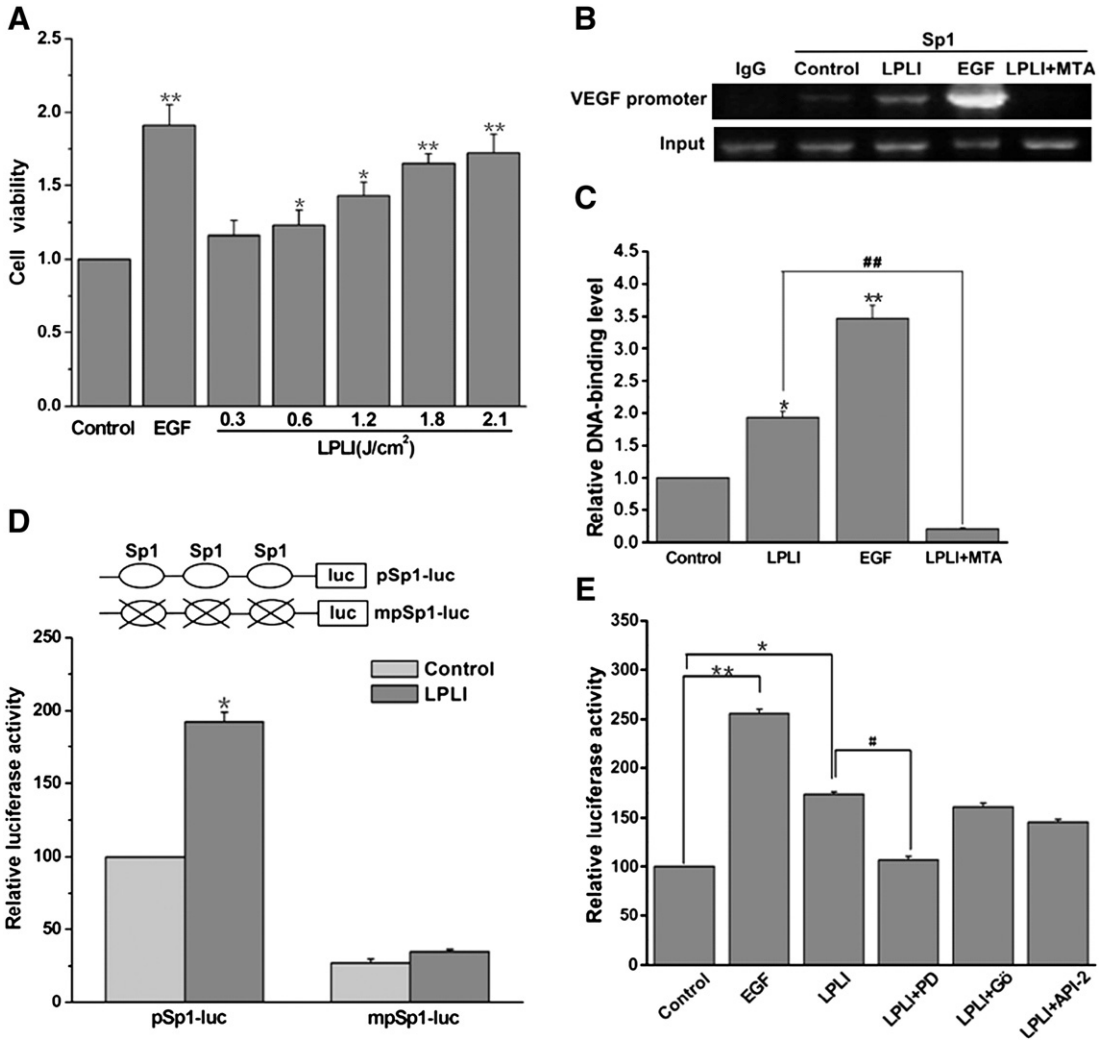

Fig. 1. LPLI enhances transcriptional activity of Sp1 dependent on ERK, but independent on PKC-ζ or Akt. (A) HUVEC-CS cells were seeded on 96-well microplates for 24 h and then irradiated with He–Ne laser at dose of 0.3, 0.6, 1.2, 1.8 and 2.1 J/cm^2, respectively or treated with 50 ng/ml EGF. Cell viability was assessed by the CCK-8 assay after 24 h. Data represent mean ± SEM (n = 3; $^{*}P<0.05$, $^{*}P<0.01$ *vs.* control cells). (B) ChIP assay was done to examine DNA-binding activity of Sp1 to VEGF promoter in cells received different treatments in HUVEC-CS cells. (C) Quantitative analysis of DNA-binding levels of Sp1. Data represent mean ± SEM (n = 3; $^{*}P<0.05$, $^{**}P<0.01$ *vs.* control cells, $^{\#\#}P<0.01$ *vs.* indicated cells). (D) Luciferase reporters pSp1-luc and mpSp1-luc were transiently transfected into HEK 293T cells. Relative luciferase activity assay in cells received different treatments was performed. Data represent the mean ± SEM (n = 3; $^{*}P<0.05$ *vs.* control cells). (E) HEK 293T cells transfected with pSp1-luc were pretreated with PD, Gö and API-2 for 30 min before LPLI. Relative luciferase assay was performed. Data represent mean ± SEM (n = 3; $^{*}P<0.05$, $^{**}P<0.01$ *vs.* control cells, $^{\#}P<0.05$ *vs.* indicated cells).

showed that LPLI treatment led to the translocation of ERK from cytoplasm to nucleus.

ERK is usually activated by phosphorylation, thus, western blot was performed to detect the phosphorylation of ERK. We found that the level of ERK phosphorylation was elevated at 30 min after LPLI in whole cell lysate (WCL). Similar results were obtained in cells treated with EGF, with a more rapid and higher level of ERK phosphorylation (Fig. 2F, G). Meanwhile, the phosphorylation of ERK in nucleus was also showing a progressive level at 1 h after LPLI, lasting for the next 3 h (Fig. 2H, I). Taken together, these results strongly proved that LPLI effectively induced ERK activation and nuclear translocation due to its phosphorylation.

3.3. Activated ERK upon LPLI interacts with Sp1 and activates it through phosphorylation

To further confirm whether Sp1 phosphorylation is affected by ERK upon LPLI, the level of Sp1 phosphorylation on Thr453 and Thr739 was evaluated. Western blot analysis manifested that the level of Sp1

Fig. 2. LPLI induces ERK activation and its translocation from cytoplasm to nucleus. (A) MEK-YFP and ERK-CFP plasmids were co-transfected into HUVEC-CS cells. The fluorescence images of CFP and FRET channels excited by Ar–Ion laser (458 nm) and FRET/CFP ratio were recorded with LSM microscope. The decreased ratio of FRET/CFP indicates the activation of ERK. (B) Quantitative analysis of CFP, FRET intensities and the ratio in single cell treated with LPLI corresponding to the images in A. (C) Quantitative analysis of relative FRET/CFP ratio in cells received different treatments. (D) Representative time-series images of ERK-YFP after different treatments (n = 5). (E) Quantitative analysis of ERK-YFP fluorescence intensities in nucleus of cells subjected to different treatments. The data represent mean ± SEM of three independent experiments (10 cells per condition). (F) Representative western blot assay for detecting the levels of ERK phosphorylation after LPLI treatment in whole cell lysates. (G) Quantitative analysis of phospho-ERK levels. Data represent mean ± SEM (n = 3; $^{*}P<0.05$, $^{**}P<0.01$ *vs.* control cells, $^{\#\#}P<0.01$ *vs.* indicated cells). (H) Representative western blot assay for detecting the levels of ERK phosphorylation after LPLI treatment in cytoplasm and nuclear lysates, respectively (n = 3). (I) Quantitative analysis of phospho-ERK levels. Data represent mean ± SEM (n = 3; $^{*}P<0.05$, $^{\#}P<0.05$ *vs.* control cells).

phosphorylation on Thr453 and Thr739 was elevated in endothelial cells after LPLI treatment. However, the phosphorylation was inhibited by PD (Fig. 3A, B), while both Gö and API-2 caused little effect on the phosphorylation of Sp1. The similar result was also obtained in HEK 293T cells. Taken together, these results showed that LPLI effectively promoted Sp1 activation due to its phosphorylation on Thr453 and Thr739 through the activation of ERK.

To further determine whether Sp1 transcriptional activity is regulated by ERK, we explored the dynamic interaction between Sp1 and ERK. Cells were transiently co-transfected with CFP-Sp1 and ERK-YFP.

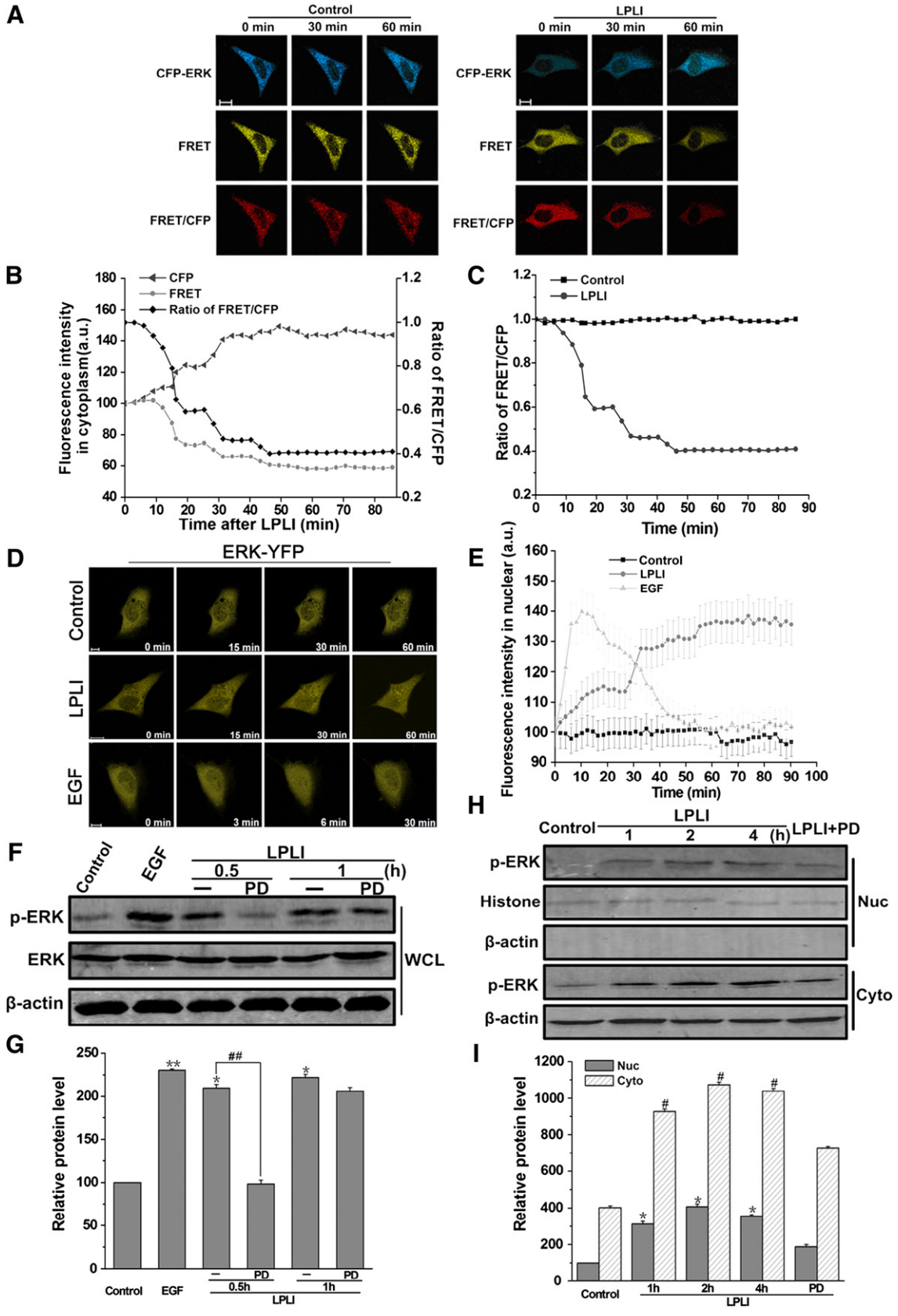

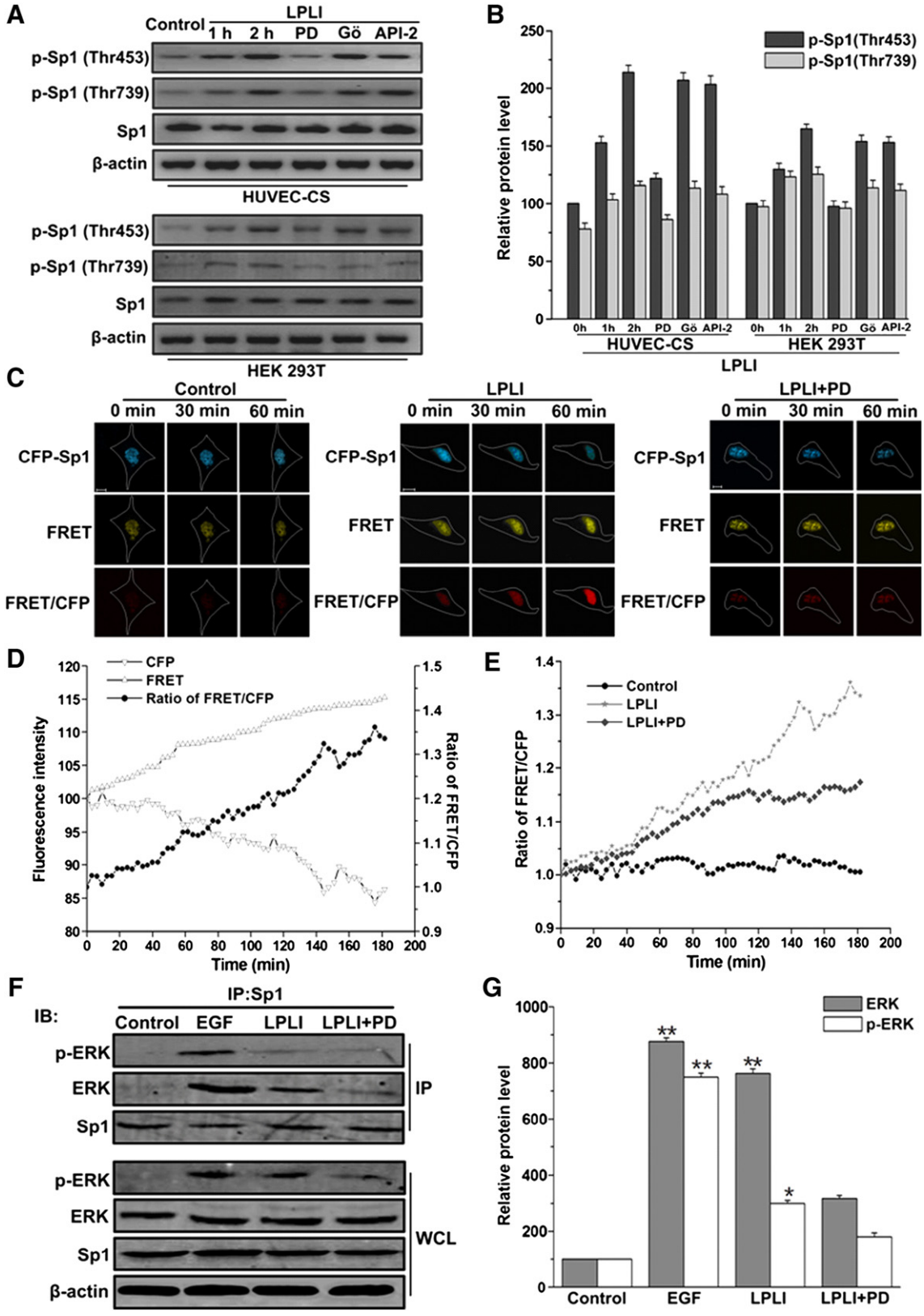

Fig. 3. Activated ERK upon LPLI interacts with Sp1 and activates it through phosphorylation. (A) Representative western blot assay for detecting the levels of Sp1 phosphorylation (Thr453 and Thr739) received different treatments. (B) Quantitative analysis of phospho-Sp1 levels. Data represent mean ± SEM. (C) CFP-Sp1 and ERK-YFP plasmids were co-transfected into HUVEC-CS cells. The real-time CFP, FRET and the ratio of FRET/CFP fluorescence images were collected with LSM510 microscopy. (D) and (E) Quantitative analysis of CFP, FRET and the ratio in single cell treated with LPLI and of relative FRET/CFP emission ratio in cells received indicated treatments. (F) Co-IP with anti-Sp1 antibody was used to pull-down ERK and phospho-ERK after LPLI treatment with or without PD. Western blot for ERK and phospho-ERK showed the amounts of ERK and phospho-ERK binding to Sp1 in IP and WCL. Similar results were obtained from three independent experiments. (G) Quantitative analysis of ERK and phospho-ERK levels. Data represent mean ± SEM (n = 3; $^{*}P<0.05$, $^{**}P<0.01$ *vs.* control cells).

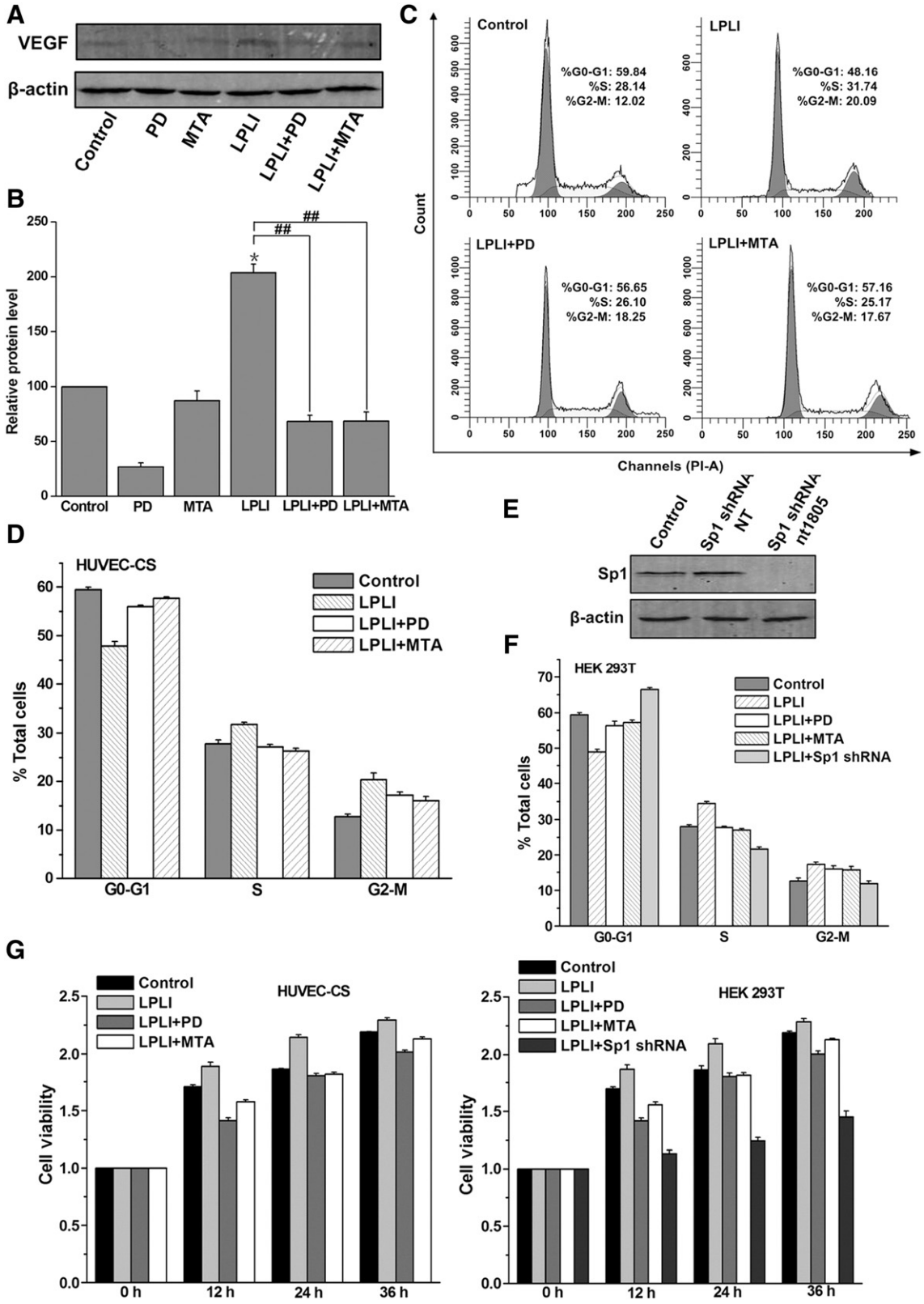

Fig. 4. LPLI promotes VEGF expression, the transition from G1- to S-phase and proliferation through activating ERK/Sp1. (A) Representative western blot assay for detecting the levels of VEGF expression after cells were subjected to different treatments. Similar results were obtained from three independent experiments. (B) Quantitative analysis of VEGF levels. Data represent mean ± SEM (n = 3; $^{*}P<0.05$ *vs.* control cells, $^{\#\#}P<0.01$ *vs.* indicated cells). (C) FACS analysis to classify each cell cycle. Quantitation of every phase by PI staining was performed. Representative images were shown. (D) and (F) Quantitative analysis of all phases. Data represent mean ± SEM of three independent experiments. (E) Representative western blot assay for detecting the levels of Sp1 expression after cells interfered by Sp1-shRNA nt1805. (G) Cell viability was assessed by CCK-8 assay. Data represent mean ± SEM of three independent experiments.

The fluorescence images of CFP, FRET and the ratio of FRET/CFP were shown in Fig. 3C–E. The CFP fluorescence decreased, while the FRET increased and the FRET/CFP ratio also ascended in LPLI-treated cells (Fig. 3C), representing the increased interaction between Sp1 and ERK. However, the ascended trend of ratio was inhibited when cells were exposed to PD before LPLI, indicating that the interaction between CFP-Sp1 and ERK-YFP was suppressed. In control cells, the ratio remained unchanged (Fig. 3C). The quantitative analysis of the fluorescence intensities was shown in Fig. 3D and E.

In parallel, Co-IP was performed to confirm the interaction between Sp1 and ERK. The results showed that the amounts of ERK and phospho-ERK that bound to Sp1 increased significantly in response to LPLI, which was inhibited in the presence of PD (Fig. 3F, G). The level of p-ERK in the whole cell lysate was also increased in response to LPLI, which was reversed by PD significantly, consisting with Fig. 2F and G. Therefore, these results demonstrated that LPLI promoted the interaction between ERK and Sp1 to mediate the phosphorylation of Sp1.

3.4. LPLI promotes VEGF expression, the transition from G1- to S-phase and proliferation through activating ERK/Sp1

In order to explore the effects of Sp1 activation induced by LPLI on cells, we detected the expression of VEGF in various treatment groups. As shown in Fig. 4A, VEGF expression increased following LPLI compared to non-treated cells. However, it decreased remarkably in cells pretreated with PD or MTA before LPLI, revealing that LPLI upregulated VEGF expression through ERK/Sp1 pathway. Relative protein level was shown in Fig. 4B.

To determine the influence of ERK/Sp1 pathway on cell cycle, FACS analysis was used to classify each cell cycle. We found that the percentage of cells in G0/G1-phase reduced about 11% whereas it increased in S- and G2/M-phase after LPLI, suggesting that LPLI promoted the transition of G0/G1- to S-phase (Fig. 4C–D, F). However, pretreatment with PD or MTA before LPLI made G0/G1-phase increase about 8% and S-phase 6% compared with LPLI-treated cells, leading to cell cycle arrest in G0/G1-phase. Meanwhile, when Sp1 expression was interfered with Sp1-specific targeting shRNA nt1805 in 293T cells (Fig. 4E), cell cycle accelerated by LPLI was also inhibited largely (Fig. 4F), showing that LPLI triggered an accelerated progression from G1- to S-phase depending on ERK/Sp1 pathway. A complete understanding of all cell cycle check points is critical for the identification of new therapeutic targets for the development of regenerative technologies. Furthermore, cell viability was also examined to affirm the role of ERK/Sp1 pathway playing in proliferation (Fig. 4G). Cell proliferation was speeded up by LPLI, which was reversed by PD or MTA or Sp1-silencing. Therefore, ERK/Sp1 pathway was absolutely necessary in LPLI-induced proliferation.

4. Discussion

Angiogenesis is a complicated process depending on the balance of pro- and anti-angiogenic factors that influence the quiet or proliferative state of the endothelium in a wide variety of disease [1–3]. Endothelial cells in adult mammals are among the least proliferative cell types, which are rapidly reversed in response to growth factors during pathological vascularization [49]. In recent years LPLI has been demonstrated to positively influence cellular proliferation for the process of angiogenesis on endothelial cells [18,50]. The results in the present study also showed that LPLI (632.8 nm) at a dose of 1.8 J/cm^2 significantly promoted HUVEC-CS proliferation (Fig. 1A). However, few studies have been performed to explore the underlying mechanisms. Therefore, bio-modulation mechanisms by LPLI have been the focus of intensive research.

Our previous researches have shown that cell proliferation following LPLI involves RTK/PKCs pathway, ROS/Src pathway, and PI-3K/Akt pathway in COS-7 cells [51–53]. However, the mechanisms investigated before are restricted in the upstream protein kinases, which are not direct effectors in proliferation. These kinases need to activate downstream transcription factors implicated in the control of cell proliferation.

Sp1 is critical for the regulation of fundamental cellular processes, including cell proliferation, survival and angiogenesis [54] through transcriptional regulation of genes, and its knockout in mice results in embryonic lethality. It was shown to stimulate transcription through binding to GC-rich boxes present on a large body of promoters [25–27]. Among the proangiogenic factors identified so far, VEGF needed for proliferation and survival of endothelial cells represents one of the most potent stimuli of vascularization. Previous study has identified the proximal GC-rich box (−88/−50) of the VEGF promoter bound by Sp1 is the main target for growth factors stimulation [29]. Our finding indicated that LPLI enhanced DNA-binding activity of Sp1 to VEGF promoter, which was reversed by inhibition of Sp1 via mithramycin-A (Fig. 1B). Furthermore, LPLI induced VEGF production at the protein level dependent on Sp1 (Fig. 4A). Luciferase assays also displayed that transactivation activity of Sp1 increased responding to LPLI (Fig. 1D). Sp1 is regulated through changing its phosphorylation level by Akt, PKC-ζ and ERK. We found that the inhibition of ERK activity suppressed transactivation of Sp1 induced by LPLI (Fig. 1D). These results suggested that ERK was activated by LPLI, with translocating from cytoplasm to nucleus and subsequently targeted Sp1 to regulate its transcription.

MAP kinase pathways are evolutionarily conserved signaling modules by which cells transduce extracellular signals into intracellular responses. The prototypical MAP kinase pathway is the Ras-dependent ERK pathway activated preferentially by mitogenic factors, differentiation stimuli and cytokines to regulate activity and/or expression of other proteins [55,56]. ERK is necessary for G1- to S-phase progression and is associated with induction of positive regulators of the cell cycle and inactivation of antiproliferative genes [57]. In quiet state, ERK mainly locates in cytoplasm anchored by their association with the MAPK/ERK kinases (MEKs) and several other proteins. Once activated, ERK partly translocates from cytoplasm to nucleus [58] to phosphorylate abroad substrates distributing throughout different subcellular compartments, including the cytoplasm and the nucleus. Previous research has proved that LPLI induces the activation and proliferation of quiescent satellite cells and delays their differentiation through MAPK/ERK pathway [59]. However, there has been no evidence about ERK activation in response to LPLI in endothelial cells. So in our study, three different physical–chemical methods were used to investigate the effect of LPLI on ERK in human endothelial cells. ERK-YFP translocation assay, FRET technology and western blot analysis of ERK phosphorylation all showed that ERK was activated by LPLI (Fig. 2). Meantime, our results also demonstrated that LPLI heightened the interaction between ERK and Sp1, which enhanced the phosphorylation level of Sp1 at Thr453 and Thr739 (Fig. 3).

Several studies have reported ERK plays a critical role in the transcription of VEGF gene following Ras transformation and growth factors and other stimuli [60]. In this study, we found that LPLI-induced VEGF production was suppressed by inhibiting the activity of ERK, as well as Sp1 (Fig. 4A, B), illustrating the expression of VEGF after LPLI was regulated by ERK/Sp1 pathway, which may be associated with the cell proliferation event and angiogenesis. Selectively inhibiting of ERK or Sp1 prevented cell cycle progression and proliferation upon LPLI (Fig. 4C–G). Thus, the above results created a general idea that LPLI promoted proliferation and angiogenesis through activating ERK/Sp1 pathway.

In addition, Sp1 participates in the regulation of gene expression sometimes through the interaction with other transcription factors and/or cofactors such as CREB-binding protein, p300, or Sp3 [61,62], representing an important transcriptional control mechanism. The phosphorylation of Sp1 on Thr453 and Thr739 may

allow the recruitment of one or more Sp1 partners required for efficient transcription. Studies on this aspect will be going on in our future work.

In summary, we propose a pathway involving LPLI-induced Sp1 activation dependent on ERK activation, through which LPLI exerts its function on driving VEGF expression and promoting proliferation of vascular endothelial cells, as one of the molecular links bridging LPLI and angiogenesis (Fig. 5). Our research raises the possibility that develops the therapeutic potential of LPLI for regulating muscle injury, wound healing and vascular regeneration. However, the precise molecular mechanisms responsible still poorly defined, so further studies should be conducted to clarify the signaling pathways involved in LPLI, providing new clue for its clinical application for diseases.

Acknowledgment

This research is supported by the National Basic Research Program of China (2011CB910402; 2010CB732602), the Program for Changjiang Scholars and Innovative Research Team in University (IRT0829), and the National Natural Science Foundation of China (30870676; 30870658). We thank Prof. Shih-Ming Huang (Graduate Institute of Life Sciences, National Defense Medical Center, Taipei, China) for kindly providing pSp1-luc and mpSp1-luc reporter genes; Prof. Jane Azizkhan-Clifford (Department of Biochemistry and Molecular Biology, Drexel University College of Medicine, Philadelphia, PA) for kindly providing Sp1-shRNA nt1805 and nontargeting control Sp1-shRNA NT; Prof. Stephen Safe (Departments of Veterinary Physiology and Pharmacology, Texas A&M University System Health Science Center, Houston, Texas) for kindly providing CFP-Sp1 plasmid; Prof. Michiyuki Matsuda (Department of Signal Transduction, Research Institute for Microbial Diseases, Osaka University, Osaka, Japan) for kindly providing ERK-YFP, MEK-YFP and CFP-ERK plasmids.

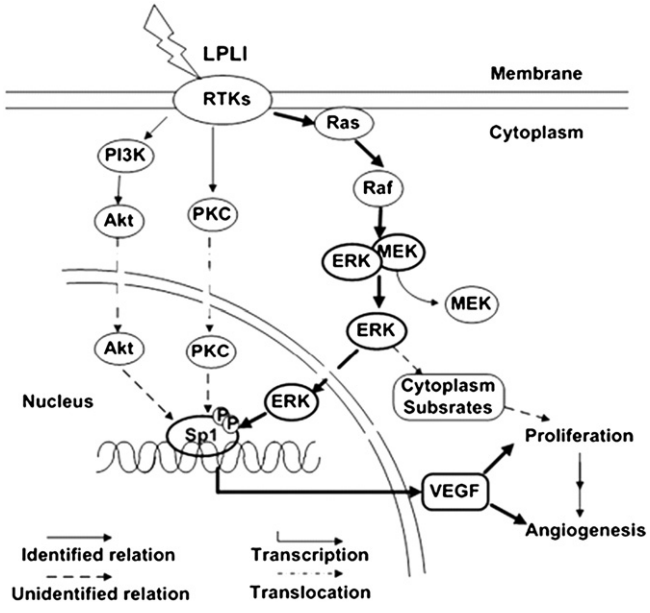

Fig. 5. Mechanism model. The model of signaling pathways activated by LPLI promoting vascular endothelial cell proliferation and angiogenesis. Activated RTKs (Receptor Tyramine Kinases) on cell membrane by LPLI induce Ras/Raf/MEK/ERK cascade response activation. Subsequently, ERK translocates from cytoplasm to nuclear where it phosphorylates Sp1 to promote Sp1-dependent transcription, increasing VEGF expression, and accelerating cell cycle progression and proliferation, which potentially facilitates angiogenesis in pathological vascularization.

References

[1] P. Carmeliet, Nature 438 (2005) 932–936.
[2] C.W. Pugh, P.J. Ratcliffe, Nature Medicine 9 (2003) 677–684.
[3] P. Romagnani, L. Lasagni, F. Annunziato, M. Serio, S. Romagnani, Trends in Immunology 25 (2004) 201–209.
[4] M. Potente, H. Gerhardt, P. Carmeliet, Cell 146 (2011) 873–887.
[5] Y. Suarez, W.C. Sessa, Circulation Research 104 (2009) 442–454.
[6] H.M. Eilken, R.H. Adams, Current Opinion in Cell Biology 22 (2010) 617–625.
[7] G. Shefer, T.A. Partridge, L. Heslop, J.G. Gross, U. Oron, O. Halevy, Journal of Cell Science 115 (2002) 1461–1469.
[8] A. Stein, D. Benayahu, L. Maltz, U. Oron, Photomedicine and Laser Surgery 23 (2005) 161–166.
[9] D. Taniguchi, P. Dai, T. Hojo, Y. Yamaoka, T. Kubo, T. Takamatsu, Lasers in Surgery and Medicine 41 (2009) 232–239.
[10] N. Ben-Dov, G. Shefer, A. Irintchev, A. Wernig, U. Oron, O. Halevy, Biochimica et Biophysica Acta 1448 (1999) 372–380.
[11] X. Gao, D. Xing, Journal of Biomedical Science 16 (2009) 4–19.
[12] L. Zhang, Y. Zhang, D. Xing, Journal of Cellular Physiology 224 (2010) 218–228.
[13] H.S. Antunes, A.M. de Azevedo, L.F. da Silva Bouzas, C.A. Adao, C.T. Pinheiro, R. Mayhe, L.H. Pinheiro, R. Azevedo, V. D'Aiuto de Matos, P.C. Rodrigues, I.A. Small, R.A. Zangaro, C.G. Ferreira, Blood 109 (2007) 2250–2255.
[14] J.A. Zivin, G.W. Albers, N. Bornstein, T. Chippendale, B. Dahlof, T. Devlin, M. Fisher, W. Hacke, W. Holt, S. Ilic, S. Kasner, R. Lew, M. Nash, J. Perez, M. Rymer, P. Schellinger, D. Schneider, S. Schwab, R. Veltkamp, M. Walker, J. Streeter, Stroke 40 (2009) 1359–1364.
[15] P.C. Silveira, L.A. Silva, T.P. Freitas, A. Latini, R.A. Pinho, Lasers in Medical Science 26 (2011) 125–131.
[16] L. Zhang, D. Xing, D. Zhu, Q. Chen, Cellular Physiology and Biochemistry 22 (2008) 215–222.
[17] H. Zhang, S. Wu, D. Xing, Cellular Signalling 24 (2012) 224–232.
[18] C.H. Chen, H.S. Hung, S.H. Hsu, Lasers in Surgery and Medicine 40 (2008) 46–54.
[19] E. Grinstein, F. Jundt, I. Weinert, P. Wernet, H.D. Royer, Oncogene 21 (2002) 1485–1492.
[20] D. Nagata, E. Suzuki, H. Nishimatsu, H. Satonaka, A. Goto, M. Omata, Y. Hirata, Journal of Biological Chemistry 276 (2001) 662–669.
[21] A.R. Black, J.D. Black, J. Azizkhan-Clifford, Journal of Cellular Physiology 188 (2001) 143–160.
[22] F.S. Santiago, H. Ishii, S. Shafi, R. Khurana, P. Kanellakis, R. Bhindi, M.J. Ramirez, A. Bobik, J.F. Martin, C.N. Chesterman, I.C. Zachary, L.M. Khachigian, Circulation Research 101 (2007) 146–155.
[23] M. Gong, W. Yu, F. Pei, J. You, X. Cui, M.A. McNutt, G. Li, J. Zheng, Journal of Cellular Biochemistry 113 (2012) 329–339.
[24] D.Q. Li, S.B. Pakala, S.D. Reddy, K. Ohshiro, J.X. Zhang, L. Wang, Y. Zhang, I. Moreno de Alboran, M.R. Pillai, J. Eswaran, R. Kumar, Proceedings of the National Academy of Sciences of the United States of America 108 (2011) 8791–8796.
[25] M.R. Briggs, J.T. Kadonaga, S.P. Bell, R. Tjian, Science 234 (1986) 47–52.
[26] J.T. Kadonaga, K.R. Carner, F.R. Masiarz, R. Tjian, Cell 51 (1987) 1079–1090.
[27] J.T. Kadonaga, R. Tjian, Proceedings of the National Academy of Sciences of the United States of America 83 (1986) 5889–5893.
[28] V.M. Leppanen, A.E. Prota, M. Jeltsch, A. Anisimov, N. Kalkkinen, T. Strandin, H. Lankinen, A. Goldman, K. Ballmer-Hofer, K. Alitalo, Proceedings of the National Academy of Sciences of the United States of America 107 (2010) 2425–2430.
[29] G. Schafer, T. Cramer, G. Suske, W. Kemmner, B. Wiedenmann, M. Hocker, Journal of Biological Chemistry 278 (2003) 8190–8198.
[30] J.Y. Chuang, Y.T. Wang, S.H. Yeh, Y.W. Liu, W.C. Chang, J.J. Hung, Molecular Biology of the Cell 19 (2008) 1139–1151.
[31] N.Y. Tan, L.M. Khachigian, Molecular and Cellular Biology 29 (2009) 2483–2488.
[32] J. Milanini-Mongiat, J. Pouyssegur, G. Pages, Journal of Biological Chemistry 277 (2002) 20631–20639.
[33] Y.L. Huang, G.Y. Shi, H. Lee, M.J. Jiang, B.M. Huang, H.L. Wu, H.Y. Yang, Cellular Signalling 21 (2009) 954–968.
[34] P.P. Dwivedi, X.H. Gao, J.C. Tan, A. Evdokiou, A. Ferrante, H.A. Morris, B.K. May, C.S. Hii, Cellular Signalling 22 (2010) 543–552.
[35] I.H. Bae, M.J. Park, S.H. Yoon, S.W. Kang, S.S. Lee, K.M. Choi, H.D. Um, Cancer Research 66 (2006) 4991–4995.
[36] P. Fojas de Borja, N.K. Collins, P. Du, J. Azizkhan-Clifford, M. Mudryj, EMBO Journal 20 (2001) 5737–5747.
[37] S.A. Armstrong, D.A. Barry, R.W. Leggett, C.R. Mueller, Journal of Biological Chemistry 272 (1997) 13489–13495.
[38] T.M. Gottlieb, S.P. Jackson, Cell 72 (1993) 131–142.
[39] M.H. Wu, J.Y. Chan, P.Y. Liu, S.T. Liu, S.M. Huang, The International Journal of Biochemistry & Cell Biology 39 (2007) 413–425.
[40] A. Astrinidis, J. Kim, C.M. Kelly, B.A. Olofsson, B. Torabi, E.M. Sorokina, J. Azizkhan-Clifford, Genes, Chromosomes & Cancer 49 (2010) 282–297.
[41] K. Kim, R. Barhoumi, R. Burghardt, S. Safe, Molecular Endocrinology 19 (2005) 843–854.
[42] A. Fujioka, K. Terai, R.E. Itoh, K. Aoki, T. Nakamura, S. Kuroda, E. Nishida, M. Matsuda, Journal of Biological Chemistry 281 (2006) 8917–8926.
[43] S.M. Gifford, M.A. Grummer, S.A. Pierre, J.L. Austin, J. Zheng, I.M. Bird, Journal of Endocrinology 182 (2004) 485–499.
[44] J.M. Cale, I.M. Bird, Biochemical Journal 398 (2006) 279–288.
[45] A. Rettino, F. Rafanelli, G. Genovese, M. Goracci, R.A. Cifarelli, A. Cittadini, A. Sgambato, American Journal of Physiology. Cell Physiology 297 (2009) C1113–C1123.
[46] J.A. Stirland, J.D. Johnston, F.R. Cagampang, P.J. Morgan, M.G. Castro, M.R. White, J.R. Davis, A.S. Loudon, Journal of Neuroendocrinology 13 (2001) 147–157.

[47] Y. Zhang, D. Xing, L. Liu, Molecular Biology of the Cell 20 (2009) 3077–3087.
[48] L. Liu, Z. Zhang, D. Xing, Free Radical Biology & Medicine 51 (2011) 53–68.
[49] B. Hobson, J. Denekamp, British Journal of Cancer 49 (1984) 405–413.
[50] A. Schindl, H. Merwald, L. Schindl, C. Kaun, J. Wojta, British Journal of Dermatology 148 (2003) 334–336.
[51] X. Gao, T. Chen, D. Xing, F. Wang, Y. Pei, X. Wei, Journal of Cellular Physiology 206 (2006) 441–448.
[52] J. Zhang, D. Xing, X. Gao, Journal of Cellular Physiology 217 (2008) 518–528.
[53] L. Zhang, D. Xing, X. Gao, S. Wu, Journal of Cellular Physiology 219 (2009) 553–562.
[54] N.M. Mazure, M.C. Brahimi-Horn, J. Pouyssegur, Current Pharmaceutical Design 9 (2003) 531–541.
[55] S.J. MacKenzie, G.S. Baillie, I. McPhee, G.B. Bolger, M.D. Houslay, Journal of Biological Chemistry 275 (2000) 16609–16617.
[56] Y. Cui, R.M. Costa, G.G. Murphy, Y. Elgersma, Y. Zhu, D.H. Gutmann, L.F. Parada, I. Mody, A.J. Silva, Cell 135 (2008) 549–560.
[57] S. Meloche, J. Pouyssegur, Oncogene 26 (2007) 3227–3239.
[58] H. Shankaran, D.L. Ippolito, W.B. Chrisler, H. Resat, N. Bollinger, L.K. Opresko, H.S. Wiley, Molecular Systems Biology 5 (2009) 332–344.
[59] G. Shefer, U. Oron, A. Irintchev, A. Wernig, O. Halevy, Journal of Cellular Physiology 187 (2001) 73–80.
[60] K.N. Meadows, P. Bryant, P.A. Vincent, K.M. Pumiglia, Oncogene 23 (2004) 192–200.
[61] Y.S. Kao, J.C. Fong, Cellular Signalling 23 (2011) 901–910.
[62] T.I. Kassimatis, A. Nomikos, I. Giannopoulou, A. Lymperopoulos, D.A. Moutzouris, I. Varakis, L. Nakopoulou, Renal Failure 32 (2010) 243–253.